Electrochemical and Solid-State Letters, **4** (10) A166-A169 (2001)
1099-0062/2001/4(10)/A166/4/$7.00 © The Electrochemical Society, Inc.

Preparation of Orthorhombic $LiMnO_2$ Material by Quenching

Yun Sung Lee* and Masaki Yoshio,z**

Department of Applied Chemistry, Saga University, 1 Honjo, Saga 840-8502, Japan

Orthorhombic $LiMnO_2$ was synthesized using LiOH and γ-MnOOH starting materials at 1000°C in an argon atmosphere by quenching method. X-ray diffraction revealed that the $LiMnO_2$ compound showed a well-defined orthorhombic phase of a space group with *Pmnm*. The lattice constants of the resulting compound were $a = 2.806$ Å, $b = 5.750$ Å, and $c = 4.593$ Å. The $LiMnO_2$ delivered 193 mAh/g in the first cycle and still delivered 183 mAh/g after 50 cycles at room temperature. We confirmed that the initial discharge capacity of $LiMnO_2$ agreed well with its specific surface area and grinding treatment was effective in improving initial cycling performance. The well-defined orthorhombic $LiMnO_2$ compound made by the quenching method exhibited an excellent cycle performance because it could maintain its original structure on cycling by suppressing transformation to the spinel structure.
 [DOI: 10.1149/1.1399879]

Manuscript received May 16, 2001. Available electronically August 16, 2001.

The layered oxide materials $LiMO_2$ (M = Co, Ni, Mn,...) and the $LiMn_2O_4$ spinel are the most widely studied 4 V cathode materials for lithium secondary batteries with high energy density.[1-3] The Mn-based materials have attracted wide attention as intercalation cathode materials because of their low cost and nontoxicity. The $LiMn_2O_4$ spinel has shown excellent cycle performance at room temperature in the 4 V region. However, it presented a significant capacity loss when cycled in the (3 + 4) V region as well as at high temperature.[4,5] The tetragonal to cubic structure occurred when the average manganese valence reached about 3.5. It is the critical concentration of Mn^{3+} that leads to the Jahn-Teller distortion.[6] $LiMnO_2$ (both orthorhombic and monoclinic) materials exhibit better cycle performances than the $LiMn_2O_4$ spinel when used over a wide voltage region.[7,8]

Orthorhombic $LiMnO_2$ (herein referred to as o-$LiMnO_2$) of the ordered rock salt structure described by Johnston and Keikes[9] and Hoppe *et al.*[10] has been studied by many research groups.[11-22] The low temperature synthesis (170-450°C) first reported by Ohzuku *et al.* showed a large rechargeable capacity above 190 mAh/g using lithium hydroxide and manganite (γ-MnOOH) at 450°C.[11] Reimers *et al.* also reported a new synthetic method, an ion exchange technique, and revealed an irreversible structural change to the spinel phase using *in situ* X-ray diffraction (XRD).[12]

Croguennec *et al.* and other groups reported a mild synthetic route at midrange temperatures (600-750°C).[14-19] They contributed to revealing the capacity loss mechanism and improving the cyclability of the o-$LiMnO_2$ material. However, the results showed a reduced initial discharge capacity (about 130 mAh/g) and some problems such as an unstable charge valence.[16-18] Furthermore, the elevated temperature performance of o-$LiMnO_2$ has not been reported.

Davidson *et al.* and Jang *et al.* also reported the synthesis of o-$LiMnO_2$ material by a high temperature synthetic method (>900°C).[20-22] Specifically, Jang *et al.* successfully synthesized o-$LiMnO_2$ material using LiOH and Mn_3O_4 under a reduced oxygen atmosphere, which exhibited an excellent cyclability between 4.4 and 2.0 V at room temperature. They first reported the high temperature performance at 55°C and observed a nanodomain structure in $LiMnO_2$ using transmission electron microscopy (TEM) and high resolution electron microscopy (HREM) which was produced by a cycling-induced phase transformation. The capacity loss of o-$LiMnO_2$ at high temperature was much larger than that during the room temperature test.[22]

From a review of previous studies, we found the following problems: first was the complexity of the synthetic process. For low temperature synthesis, most cases used an excess amount of lithium salt or lithium/sodium exchange reaction to form the homogeneous $LiMnO_2$ phase. It requires a long reaction time and other reaction steps. Even for high temperature synthesis, very sensitive synthetic conditions and some treatments to improve the reaction between the starting materials are needed. Second, there is no report showing a good cycle performance of o-$LiMnO_2$ at high temperature. And last, o-$LiMnO_2$, which was synthesized at high temperature, needed enough time to reach the maximum discharge capacity at room temperature. Although it critically depends on current density and the cycle test conditions, this indication is not desirable to use this cathode material for lithium secondary batteries.

Recently, we reported that the $LiAl_{0.1}Mn_{1.9}O_4$ material using LiOH and γ-MnOOH showed a good cyclability both in the 3 and 4 V regions.[23-25] Furthermore, tetragonal $Li_2Mn_2O_4$ material, which was synthesized using LiI as a reducing agent, showed not only a high discharge capacity over 200 mAh/g, but also good cycle performance in the (3 + 4) V region.[26] Based on our previous research, we successfully synthesized a new type of o-$LiMnO_2$ material using LiOH and γ-MnOOH by a quenching method. In this paper, we report the synthetic method and physicochemical characterizations of o-$LiMnO_2$, which can satisfy all three aspects at the same time.

Experimental

The o-$LiMnO_2$ material was synthesized using $LiOH \cdot H_2O$ (Osaka Kisida Chemical, Japan) and γ-MnOOH (Tosoh Chemical, Japan). The mixture of LiOH and γ-MnOOH (molar ratio of Li/Mn = 1.02) was thoroughly ground in an agate. It was pressed at 300 kg/cm^2 pressure into a 25 mm diam pellet to improve the reactivity between particles of the precursor. The pellet was calcined at 950-1100°C for 10 h in an argon atmosphere.

The powder X-ray diffraction (XRD, Rint 1000, Rigaku) using Cu Kα radiation was employed to identify the crystalline phase of the synthesized materials. The lithium and manganese concentrations in the resulting materials were analyzed using an inductively coupled plasma spectrometer (ICP, SPS 7800, Seiko Instruments, Japan). The specific surface area was measured in a Gemini 2375 instrument using the Brunauer, Emmett, and Teller (BET) method. The particle morphologies of the resulting compound were observed using a scanning electron microscope (SEM, JSM-5300E, Japan Electron, Ltd., Japan).

The electrochemical characterizations were performed using CR2032 coin-type cells. The cathode was fabricated with 20 mg of accurately weighed active material and 12 mg of conductive binder

* Electrochemical Society Student Member.
** Electrochemical Society Active Member.
z E-mail: yoshio@ccs.ce.saga-u.ac.jp

(8 mg of Teflonized acetylene black (TAB) and 4 mg of graphite). It was pressed on a 250 mm^2 stainless steel mesh used as the current collector at 300 kg/cm^2 and dried at 200°C for 5 h in an oven. The test cell was made of a cathode and a lithium metal anode (Cyprus Foote Mineral Co.) separated by a porous polypropylene film (Celgard 3401). The electrolyte used was a mixture of 1 M $LiPF_6$-ethylene carbonate (EC)/dimethyl carbonate (DMC) (1:2 by volume) (Ube Chemical, Japan). All assembling of the cell was carried out in an argon-filled dry box. The charge and discharge cycling was performed galvanostatically at a current density of 0.4 mA/cm^2 with a cutoff voltage of 2.0-4.5 V (*vs.* Li/Li^+) at room and high temperatures (50°C).

Results and Discussion

Phase analysis of the $LiMnO_2$ compound.—The chemical analysis showed that the powder composition was $Li_{0.98}Mn_{0.99}O_2$. o-$LiMnO_2$ was obtained from the calcination at 950-1100°C for 10 h in an argon atmosphere by rapid cooling. The effect of the cooling method is discussed in the next paragraph. We emphasize that $LiMnO_2$ in this study was synthesized by a one-step method without intermediate regrinding or other treatments. From the thermal analysis, it showed another reaction about 950°C, which converts the $LiMn_2O_4$ synthesized at about 800°C to the orthorhombic $LiMnO_2$ compound. Figure 1 shows the XRD pattern of the $LiMnO_2$ materials calcined at various calcination temperatures. For calcination temperature $T<950$°C, it showed mixed structure patterns with a cubic phase and a tetragonal phase in the XRD diagram. However, when the calcination temperature is above 950°C (Fig. 1a), the (010) peak at $2\theta = 15.4°$ was rapidly increased and other peaks also indicated a major phase of the o-$LiMnO_2$ material. For the 1050°C sample, it exhibited a pure XRD pattern without other impurities and a very small amount of the Li_2MnO_3 phase. However, the intensity ratios of (110)/(021) and (002)/(120) in this compound were opposite that of the 1000°C powder. The 1100°C sample (Fig. 1d) presented a very different XRD pattern with a strong Li_2MnO_3 impurity peak and a smaller (011) peak. Although the difference in the intensity ratios of the (110)/(021) and (002)/(120) peaks between 1000 and 1050°C samples could not be explained until now, we considered that the well-ordered o-$LiMnO_2$ material was formed at the calcination temperatures of 1000-1050°C.

The effect of different cooling methods.—To investigate the effect of the cooling method, two $LiMnO_2$ pellets were calcined at 1000°C for 10 h under an argon atmosphere in the same box-furnace. One pellet was removed from the furnace and quenched directly in air; the other remained in the furnace and was cooled slowly. The cooling rate was 5°C/min.

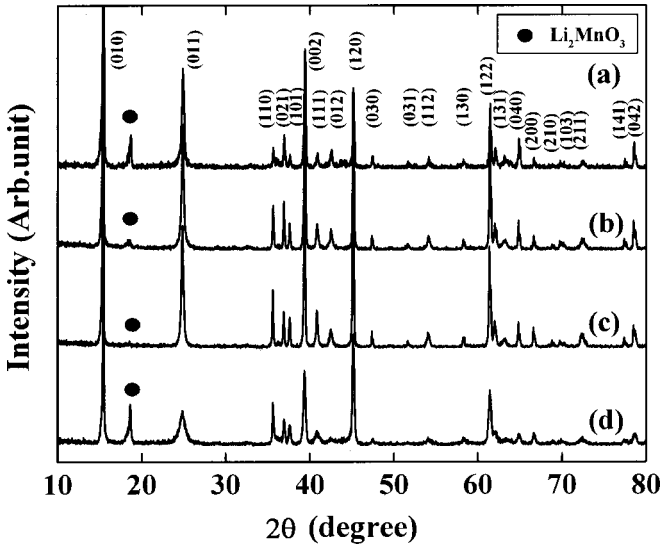

Figure 1. XRD patterns of $LiMnO_2$ material (a) 950, (b) 1000, (c) 1050, and (d) 1100°C.

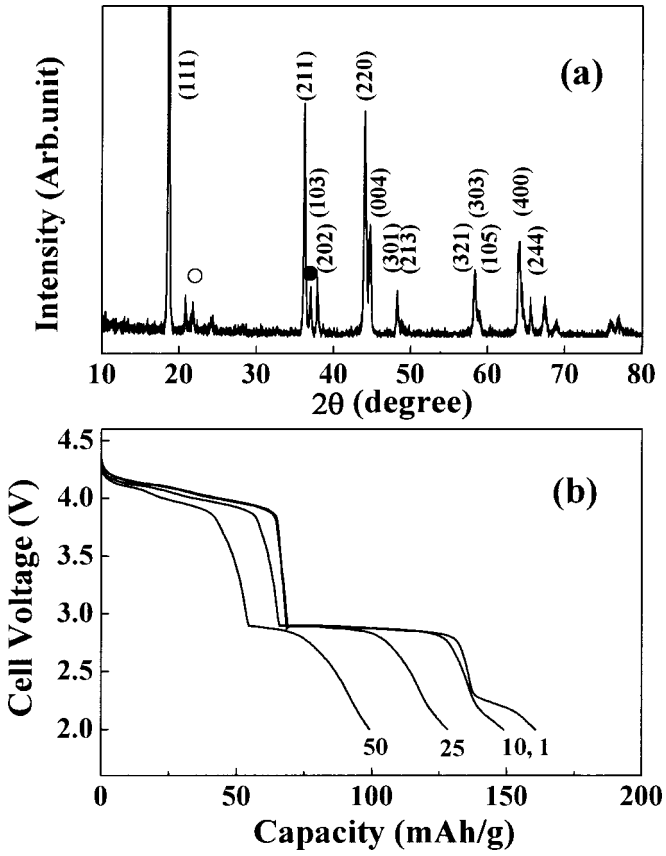

Figure 2. The characterization of $LiMnO_2$ which was synthesized by slow cooling. The cooling rate was 5°C/min (○: Mn_2O_3, ●: Li_2MnO_3).

The pellet quenched in air showed a well-defined orthorhombic phase of a *Pmnm* space group as shown in Fig. 1b. The lattice constants were $a = 2.806$ Å, $b = 5.750$ Å, and $c = 4.593$ Å, which showed a slightly large *c*-value compared with other reports.[10,11] However, the other pellet, which was synthesized by slow cooling (Fig. 2a), consisted of mixed phases of Li_2MnO_3 (monoclinic) and $LiMn_2O_4$ (spinel). This means that $LiMnO_2$ using LiOH and γ-MnOOH in this study had a structural change when it was slowly cooled in the furnace. Because the cooling rate was slow to differentiate the quenching effect, the pellet in the furnace can react continuously with oxygen during the cooling process. Tang *et al.* reported a similar result that the transformation of o-$LiMnO_2$ into the mixture of $LiMn_2O_4$ and Li_2MnO_3 was accompanied by the absorption of oxygen gas during the calcination process ($3LiMnO_2 + 1/2\ O_2 \rightarrow Li_2MnO_3 + LiMn_2O_4$).[19] Furthermore, this compound showed a similar charge/discharge curve compared with the $LiMn_2O_4$ spinel in the 4 V region. Figure 2b shows that there are two distinct plateaus, at 4.05 and 4.15 V, in the 4 V region and it exhibits almost the same discharge pattern compared with $LiMn_2O_4$ in the 3 V region except for another plateau below 2.5 V. The first discharge capacity exhibited the highest value during the 50 cycles. This is another difference compared to that of the o-$LiMnO_2$ system in this study, which showed a very low discharge capacity in the first cycle (see Fig. 3). From these results, we found that orthorhombic $LiMnO_2$ in this study could preserve its original structure by a quenching process in air, which prevented structural transformation to the spinel-like phase during the cooling process.

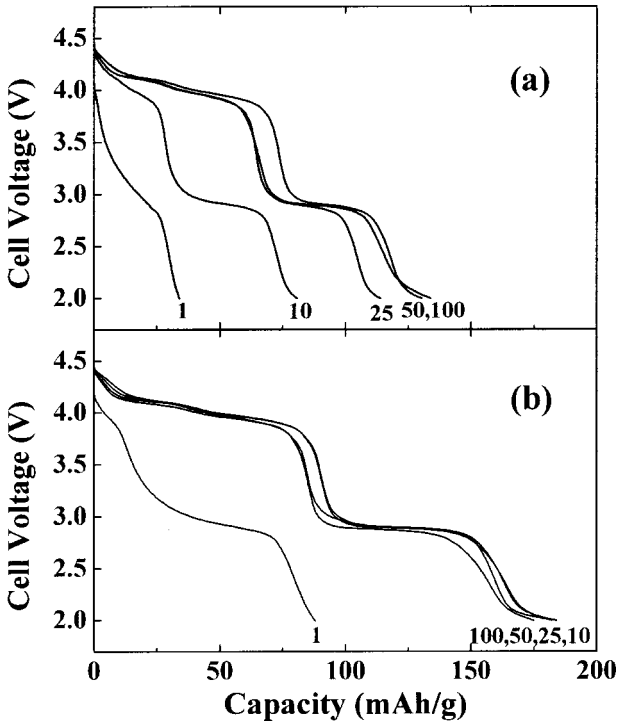

Figure 3. Discharge curves with the number of cycles for the Li/1 M $LiPF_6$-EC/DMC/$LiMnO_2$ cells. (a) 25°C test and (b) 50°C test. Cycling was carried out at a constant charge-discharge current density of 0.4 mA/cm^2 between 4.5 and 2.0 V.

Cycle behavior of o-$LiMnO_2$ material.—Figure 3 shows the discharge curves of the $LiMnO_2$ electrode as a function of the cycle number at room (25°C) and high (50°C) temperatures. The data were collected at a current density of 0.4 mA/cm^2 between 4.5 and 2.0 V. The $LiMnO_2$ electrode, which was cycled at room temperature, showed a very small initial discharge capacity of about 34 mAh/g and still increasing capacity on cycling. Furthermore, for the high temperature test cell, even if it also showed a small initial discharge capacity during the first cycle, the increased capacity was very fast and reached a maximum point during the early stage. Although Jang *et al.* reported a similar result for o-$LiMnO_2$, which exhibited an excellent cyclability under almost the same test conditions, the discharge capacity in high temperature continuously decreased and reached about 80 mAh/g after the 100th cycle.[22] However, the $LiMnO_2$ compound in this research delivered 186 mAh/g during the 10th cycle (maximum value of capacity) and still delivered 176 mAh/g after 100 cycles. The cycle retention rate is 95%, therefore, it only decreased by 0.1 mAh/g per cycle in the 3 and 4 V regions. Note that o-$LiMnO_2$ material obtained by quenching method presented an excellent cycle performance even for the high temperature test.

The o-$LiMnO_2$ in this study showed a wide difference in capacity between the room and high temperature test as shown in Fig. 3. However, there seems to be one common factor in the charge/discharge process. The two $LiMnO_2$ cells at different temperatures showed a similar discharge curve in the first cycle and then these changed into a spinel-like phase upon cycling. Many research groups have reported the same result, in which o-$LiMnO_2$ irreversibly transforms into a material with a spinel-like structure during cycling.[7,17,18] It is well known that this transforming induces an abrupt capacity loss in the $LiMnO_2$ system even though it improves the electrochemical performance. We also found the same result in the high temperature test cell and it clearly revealed the capacity loss mechanism in the $LiMnO_2$ system. The discharge capacity of o-$LiMnO_2$ at 50°C increases up to the 10th cycle accompanied by a spinel transformation. After reaching the maximum point, however, the capacity gradually decreased. The discharge curve for the 100th cycle and its cycle behavior were analogous to that of the cubic spinel ($LiMn_2O_4$) system.

We also found one different fact from previous reports.[11-23] The phase transformation of $LiMnO_2$ synthesized by the high temperature method (≥800°C) occurs very slowly compared with that of the compound using the lower temperature synthetic method (≤600°C). This means a high crystalline orthorhombic $LiMnO_2$ formed by high temperature synthesis could preserve its original structure on cycling and more effectively suppress transformation into the spinel structure. Specifically, $LiMnO_2$ obtained by quenching maintained its original structure much easier. Because the cooling rate was very fast, there was not enough time to react with oxygen which could induce a spinel-like transformation during cooling. Therefore, it could hold a well-developed orthorhombic phase up to room temperature and exhibit a very stable cycle performance even for the high temperature test by sustaining its original structure on cycling. A more detailed discussion about electrochemical properties and capacity loss mechanism will be reported elsewhere.

The effect of grinding process on initial capacity.—Croguennec *et al.* have suggested the effect of crystallite size on the cycle performance of $LiMnO_2$ material. They reported an interesting result

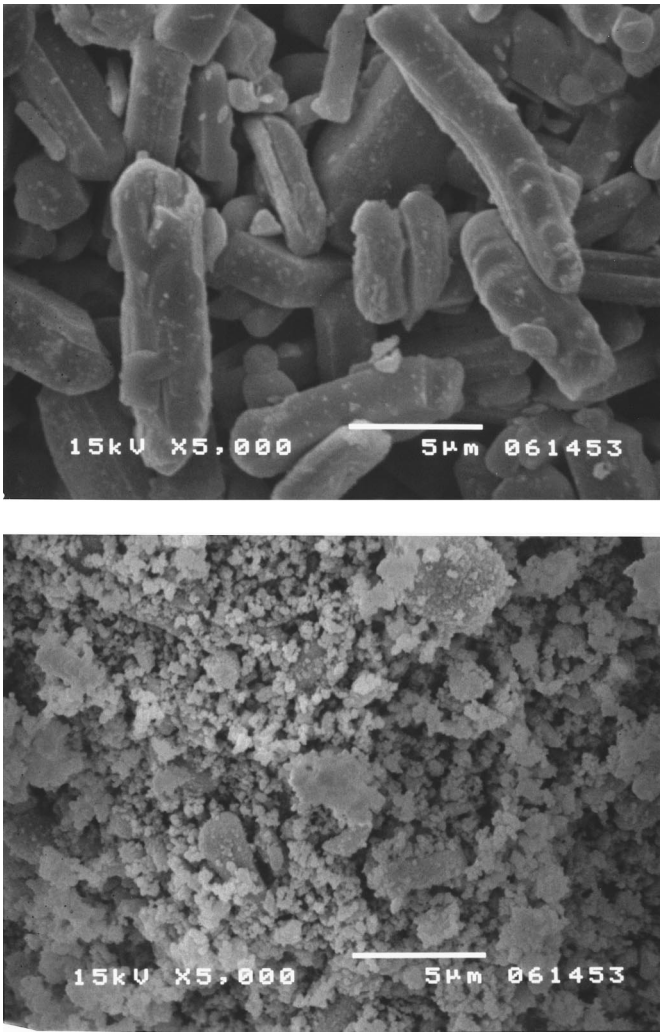

Figure 4. SEM images of $LiMnO_2$ (a) before grinding and (b) after grinding.

that the compound with small grain size showed twice the discharge capacity as a compound with large grain size.[16,17] Because the intercalation of $LiMnO_2$ compound takes place primarily on the grain surface, it prefers to have a small grain size to induce rapid lithium diffusion between the bulk and its surface. Therefore, we assume that the grinding treatment is a useful way to increase the initial discharge capacity of o-$LiMnO_2$ at room temperature. Because it showed relatively a large particle size over 10 μm as shown in Fig. 4a, the grinding treatment smashes it to small particles and increases the surface area of the o-$LiMnO_2$. Therefore, it makes better contact between the particles and electrolyte and it helps to accelerate the lithium diffusion in the $LiMnO_2$ structure. To confirm this assumption, $LiMnO_2$ was thoroughly ground in an agate mortar by a milling machine (ANM 1000, Nito. Co., Japan). Figure 4 shows the morphology of the o-$LiMnO_2$ compound using a scanning electron micrograph (SEM). The compound before grinding is represented in Fig. 4a and compared with that of the compound after grinding for 6 h (Fig. 4b). The o-$LiMnO_2$ compound before grinding had a typical bar-shape, which was shown to the compound using γ-MnOOH. The average particle size for the compound before grinding was 5-15 μm; after grinding, it was 0.5-3 μm. We could not find the whole bar-shaped type after grinding which was the original structure of $LiMnO_2$ using γ-MnOOH source. In addition, BET analysis strongly supported our assumption about the grinding effect for $LiMnO_2$ material. The surface areas of the two compounds were 0.55 m^2/g before grinding and 9.25 m^2/g after 6 h grinding, respectively. It is noticeable that the specific surface area after 6 h grinding was 17 times as much as that before grinding.

Cycle performance of o-$LiMnO_2$ depends on grinding.—To increase the initial discharge capacity of o-$LiMnO_2$ at room temperature, the resulting compound was thoroughly ground by a milling machine. Figure 5 shows the plot of specific discharge capacity *vs.* number of cycles for $LiMnO_2$ cells after 6 h grinding. As expected, it showed a very high initial discharge capacity of 193 mAh/g as well as a good cyclability at room temperature. The difference in the initial capacity between before and after grinding at room temperature is about 160 mAh/g. Although the cycle retention rate of $LiMnO_2$ after grinding at high temperature decreased to 86%, it still exhibited a pretty good cycle performance up to 50 cycles. From the results, we concluded that the grinding treatment was effective in increasing the initial discharge capacity of the $LiMnO_2$ compound at room temperature, which accelerated the rapid reaction between the particles and electrolyte.

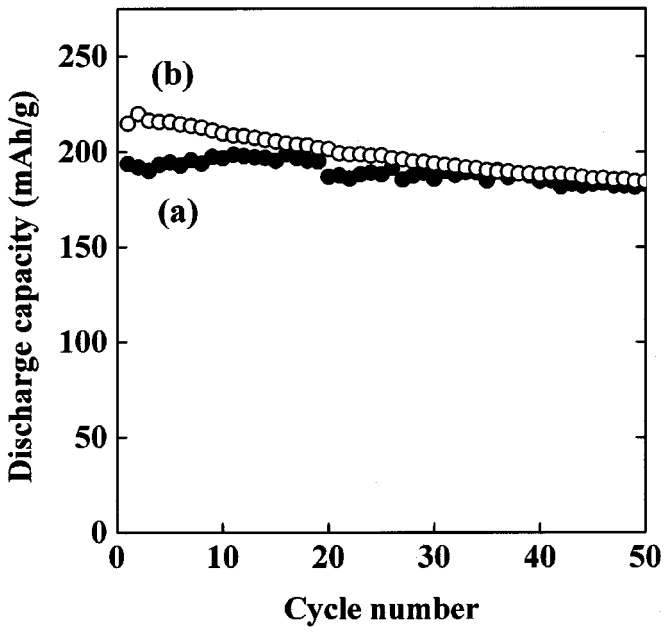

Figure 5. The plot of specific discharge capacity *vs.* number of cycles for the Li/1 M $LiPF_6$-EC/DMC/$LiMnO_2$ cells after a 6 h grinding. (a) 25°C test and (b) 50°C test. Cycling was carried out at a constant charge-discharge current density of 0.4 mA/cm^2 between 4.5 and 2.0 V.

Therefore, we succeeded in synthesizing a new type of o-$LiMnO_2$ material by quenching with an excellent cycle performance at high temperature as well as a high initial discharge capacity at room temperature. Further work is now in progress to improve the high temperature performance and more clearly reveal the mechanism of grinding effect at room temperature. These results will be reported elsewhere.

Conclusion

Orthorhombic $LiMnO_2$ was synthesized using LiOH and γ-MnOOH starting materials at 1000°C in an argon atmosphere. XRD revealed that the $LiMnO_2$ compound by quenching in air has a well-defined orthorhombic phase. It exhibited an excellent cycle performance at high temperature as well as at room temperature. However, o-$LiMnO_2$, which was synthesized at high temperature needed a long time to reach the maximum discharge capacity at room temperature. To prevent this phenomenon, it was ground by a milling machine for various times. It showed a high initial capacity above 190 mAh/g at room temperature. We confirmed that the initial discharge capacity of o-$LiMnO_2$ is strongly related to the specific surface area. The well-defined orthorhombic $LiMnO_2$ compound made by quenching exhibited excellent cycle performance even at high temperature, and can maintain its original structure during cycling and suppress transformation into the spinel structure.

Saga University assisted in meeting the publication costs of this article.

References

1. K. Mizushima, P. C. Jones, P. J. Wiseman, and J. B. Goodenough, *Mater. Res. Bull.*, **15**, 783 (1980).
2. J. R. Dahn, U. von Sacken, and C. A. Michel, *Solid State Ionics*, **44**, 87 (1990).
3. D. Guyomard and J. M. Tarascon, *Solid State Ionics*, **69**, 222 (1994).
4. J. M. Tarascon, E. Wang, and F. K. Sehokoohi, *J. Electrochem. Soc.*, **138**, 2859 (1991).
5. J. Barker, R. Koksbang, and M. Y. Saidi, *Solid State Ionics*, **82**, 143 (1995).
6. M. M. Thackeray, P. G. David, P. G. Bruce, and J. B. Goodenough, *Mater. Res. Bull.*, **18**, 461 (1983).
7. R. J. Gummow, D. C. Liles, and M. M. Thackeray, *Mater. Res. Bull.*, **28**, 1249 (1993).
8. A. R. Armstrong and P. G. Bruce, *Nature*, **381**, 499 (1996).
9. W. D. Johnston and R. R. Keikes, *J. Am. Chem. Soc.*, **78**, 3255 (1956).
10. R. Hoppe, G. Brachtel, and M. Jansen, *Z. Anorg. Allg. Chem.*, **417**, 1 (1975).
11. T. Ohzuku, A. Ueda, and T. Hirai, *Chem. Express*, **7**, 193 (1992).
12. J. N. Reimers, E. W. Fuller, E. Rossen, and J. R. Dahn, *J. Electrochem. Soc.*, **140**, 3396 (1993).
13. S. T. Myung, S. Komaba, and N. Kumagai, *Chem. Lett.*, **1**, 80 (2001).
14. P. Strobel and J. P. Levy, *J. Cryst. Growth*, **66**, 257 (1984).
15. R. J. Gummow and M. M. Thackeray, *J. Electrochem. Soc.*, **141**, 1178 (1994).
16. L. Croguennec, P. Deniard, R. Brec, and A. Lecerf, *J. Mater. Chem.*, **5**, 1919 (1995).
17. L. Croguennec, P. Deniard, R. Brec, P. Biensan, and M. Broussely, *Solid State Ionics*, **89**, 197 (1996).
18. L. Croguennec, P. Deniard, and R. Brec, *J. Electrochem. Soc.*, **144**, 3323 (1997).
19. W. Tang, H. Kanoh, and K. Ooi, *J. Solid State Chem.*, **142**, 19 (1999).
20. I. J. Davidson, R. S. McMillan, J. J. Murray, and J. E. Greedan, *J. Power Sources*, **54**, 232 (1995).
21. Y. I. Jang, B. Huang, H. Wang, D. R. Sadoway, and Y. M. Chiang, *J. Electrochem. Soc.*, **146**, 3217 (1999).
22. Y. M. Chiang, D. R. Sadoway, Y. I. Jang, B. Huang, and H. Wang, *Electrochem. Solid-State Lett.*, **2**, 107 (1999).
23. M. Okada, Y. S. Lee, and M. Yoshio, *J. Power Sources*, **90**, 196 (2000).
24. Y. S. Lee, H. J. Lee, and M. Yoshio, *Electrochem. Commun.*, **3**, 20 (2001).
25. Y. S. Lee, N. Kumada, and M. Yoshio, *J. Power Sources*, **96**, 376 (2001).
26. M. Okada, T. Mouri, and M. Yoshio, Abstract 327, The Electrochemical Society and The Electrochemical Society of Japan Meeting Abstracts, Vol. 99-2, Honolulu, HI, Oct 17-22, 1999.